RETINAL VASCULAR ABNORMALITIES IN A LARGE COHORT OF PATIENTS AFFECTED BY NEUROFIBROMATOSIS TYPE 1

A Study Using Optical Coherence Tomography Angiography

RAFFAELE PARROZZANI, MD, PhD,* ELISABETTA PILOTTO, MD,* MAURIZIO CLEMENTI, MD,†
LUISA FRIZZIERO, MD,* FRANCESCA LEONARDI, MD,* ENRICA CONVENTO, MSc,*
GIACOMO MIGLIONICO, MD,‡ SERENA PULZE, MSc,‡ PIERDAVIDE PERRINI, MD,*
EVA TREVISSON, PhD,† MATTEO CASSINA, MD,† EDOARDO MIDENA, MD, PhD*‡

Purpose: To evaluate the prevalence, the vascular features, and the clinical diagnostic implication of retinal vascular abnormalities (RVAs) associated with neurofibromatosis Type 1 (NF1) in a large cohort of patients.

Methods: Two hundred and ninety-four patients affected by NF1 were consecutively enrolled. The presence of RVAs was detected by means of infrared confocal scanning laser ophthalmoscopy images. Three hundred age- and race-matched healthy subjects were enrolled as a healthy control group. Fluorescein angiography, indocyanine green angiography, and optical coherence tomography angiography were also performed in patients with RVAs.

Results: Retinal vascular abnormalities were detected in 18 patients with NF1 (6.1%) and in none of the healthy subjects. Retinal vascular abnormalities appeared in all cases as well-defined, small, tortuous retinal vessels with a spiral aspect, originating from small tributaries of retinal veins. The presence of RVAs did not correlate with the presence of other specific ocular or systemic NF1 features ($P > 0.05$). On optical coherence tomography angiography, RVAs appeared as an isolated tortuous vessel of the superficial vascular plexus in all cases, associated with localized anomalous crowded and congested capillary network of the deep vascular plexus in 75% of cases.

Conclusion: Retinal vascular abnormalities are present in a limited proportion of patients affected by NF1 and can be considered an additional distinctive sign of the disease.

RETINA 0:1–9, 2017

The neurofibromatoses, which include neurofibromatosis Type 1 (NF1), neurofibromatosis Type 2, and schwannomatosis, are a heterogeneous group of tumor-predisposing, neurocutaneous genetic disorders.[1,2] The most common of these diseases is NF1 (1:2,700 births), which is characterized by multiple cutaneous café-au-lait spots, inguinal/axillary freckling, iris hamartomas, and neurofibromas.[1,2] This disorder is clinically diagnosed using the diagnostic criteria established by the National Institutes of Health (NIH) Consensus Development Conference.[3]

In recent years, several additional clinical features related to NF1 have been reported, including cutaneous signs (mixed vascular hamartomas and cherry angiomas, anemic nevi, juvenile xanthogranulomas, hypochromic macules, "soft touch" skin), extracutaneous findings (macrocephaly, unidentified bright objects on brain magnetic resonance imaging, and the NF1-related typical neuropsychological phenotype) and ocular signs (NF1-related choroidal abnormalities and retinal nerve fiber layer thinning in optic pathway gliomas [OPGs]).[4–8]

Neurocutaneous disorders are a group of disorders characterized by central nervous system, ocular, cutaneous, and vascular lesions of variable severity, mainly including tuberous sclerosis complex, Sturge–Weber syndrome, von Hippel–Lindau disease, and the neurofibromatoses.[3,9–11] Of these, von Hippel–Lindau and Sturge–Weber syndromes are clinically characterized by typical vascular abnormalities affecting the eye, such as retinal capillary hemangioblastoma for the former and choroidal, conjunctival, or episcleral hemangiomas for the latter.[10,11] Muci-Mendoza et al[12] first reported in 2002 a distinctive spectrum of retinal vascular abnormalities in 12 patients with NF1; they consisted of minuscule second- or third-order tortuous retinal venules. Until now, only 19 cases of NF1-related retinal vascular abnormalities (NF1-RVAs) have been reported in the literature.[12,13] Moreover, the prevalence in the NF1 population as well as the clinical and diagnostic values of this sign have never been investigated.

The aim of this study was to evaluate the prevalence and the diagnostic implications of RVAs in a large sample of consecutive patients affected by NF1. Recently, with the advent of optical coherence tomography angiography (OCT-A), it has become possible to image in vivo and separately the retinal superficial and the deep capillary plexus (SCP and DCP, respectively) in humans.[14,15] Thus, a further aim of this work was to investigate by OCT-A the different involvement of the SCP and DCP in these RVAs.

Methods

This was an observational study with prospective enrollment, compliant with the tenets of the Declaration of Helsinki. Patients were recruited from those referred between January 2015 and January 2016. Informed consent was obtained from each pediatric subject's legal guardian. Subjects older than 6 years provided assent additionally. Each patient underwent a detailed genetic, dermatologic, and ophthalmologic assessment aimed to detect and/or confirm the presence or absence of each NIH diagnostic criterion.[5,6] Briefly, café-au-lait spots, axillary or inguinal freckling, and cutaneous neurofibromas were assessed on whole skin. Both parents of pediatric patients were examined to evaluate the familial incidence. The presence of distinctive osseous lesions was also clinically examined in each patient. The presence of NF1-related systemic (extra-ocular) vascular abnormalities was investigated by direct clinical examination and anamnestic evidence, and often confirmed by ancillary tests.[5,6]

Ophthalmologic evaluation included visual acuity assessment using age-appropriate visual function tests, cycloplegic refraction, stereopsis assessment, pupillary reflex evaluation, biomicroscopy evaluation of anterior segment, air-puff tonometry in children aged older than 6 years, fundus examination using indirect ophthalmoscopy and, for cooperative patients, biomicroscopic evaluation of the optic nerve head.[5,6] The presence of Lisch nodules as a diagnostic criterion was defined as the presence of at least two Lisch nodules (NIH criteria) and was assessed using biomicroscopy.[5] The evaluation of the presence/absence of NF1-related choroidal abnormalities was obtained using Spectralis HRA + OCT (Heidelberg Engineering, Heidelberg, Germany) in near-infrared (IR) reflectance modality, after pupil dilatation, as previously reported.[5] Retinal nerve fiber layer assessment, to detect the presence of OPG, was also performed by OCT (Heidelberg Engineering), as previously reported.[6] Patients with visual acuity inferior to age-based normative data, strabismus without refractive errors, absence of stereopsis, proptosis, pathologic pupillary reflex, and those with reduced retinal nerve fiber layer thickness (obtained by OCT analysis of optic nerve head) were clinically classified as OPG suspected.[6] These patients underwent brain magnetic resonance imaging using standard procedures. Only those patients with OPG confirmed by brain magnetic resonance imaging were eventually classified as OPG affected.[6]

Inclusion criteria were as follows: patients diagnosed with NF1 according to the classic NIH criteria. Exclusion criteria were as follows: history of any ophthalmologic disease that could affect the retinal aspect (e.g., uveitis, retinopathy of prematurity, maculopathy, and congenital ocular malformations) or that could impair adequate fundus visualization (e.g., congenital cataract or other media opacities). Three hundred gender- and race-matched healthy subjects were also enrolled as a healthy control group.

Neurofibromatosis Type 1–Related Retinal Vascular Abnormalities

The presence of RVAs was evaluated using a Spectralis HRA + OCT (Heidelberg Engineering) in IR

From the *Department of Ophthalmology, University of Padova, Padova, Italy; †Clinical Genetics Unit, Department of Women and Children Health, University of Padova, Padova, Italy; ‡Ocular Oncology and Toxicology Research Unit, G.B. Bietti Foundation, IRCCS, Roma, Italy.

Reprint requests: Edoardo Midena, MD, PhD, Department of Ophthalmology, University of Padova, Via Giustiniani 2, 35128 Padova, Italy; e-mail: oncologia.tossicologia@fondazionebietti.it

reflectance modality, after pupil dilatation. The IR images of the posterior pole and the midperiphery of the retina were obtained using a 50° lens centered onto the posterior pole.[5] Retinal vascular abnormality was defined as small, tortuous retinal vessel with a "spiral/corkscrew" aspect, originating in small tributaries of retinal veins (Figure 1).[12,13] Two masked ophthalmologists evaluated each image. When detected, RVAs were studied with color fundus photography, standard (BL-) and near-IR autofluorescence (AF), fluorescein angiography (FA), indocyanine green angiography, and OCT-angiography. Fundus AF, FA, and indocyanine green angiography imaging were obtained using the Spectralis HRA-OCT (Heidelberg Engineering).

Optical Coherence Tomography Angiography

Optical coherence tomography angiography was performed using the Nidek RS-3000 Advance device (Nidek, Gamagori, Japan). This instrument has an A-scan rate of 53,000 scans per second, using a light source centered on 880 nm, with an axial and transverse resolution of 7 and 20 μm in tissue. Optical coherence tomography angiography software was used for acquisition of 3×3 mm and 6×6 mm macula cubes, with each cube consisting of 256 B-scans centered on every single RVA lesion, previously identified by IR imaging. The preset parameters were used to segment the SCP and the DCP. The preset en face images of the SCP were obtained with a slab between a segmentation line at 8 μm below the internal limiting membrane to the inner boundary of the inner nuclear layer (as identified by automated segmentation). The preset en face images of the DCP were obtained with a slab including from the inner boundary of the inner nuclear layer to 88 μm below. Moreover, the en face image of the full capillary bed was displayed, placing automatically the boundaries at the inner limiting membrane and at the retinal pigment epithelium.[16] All images were reviewed to confirm accurate segmentation by the automated
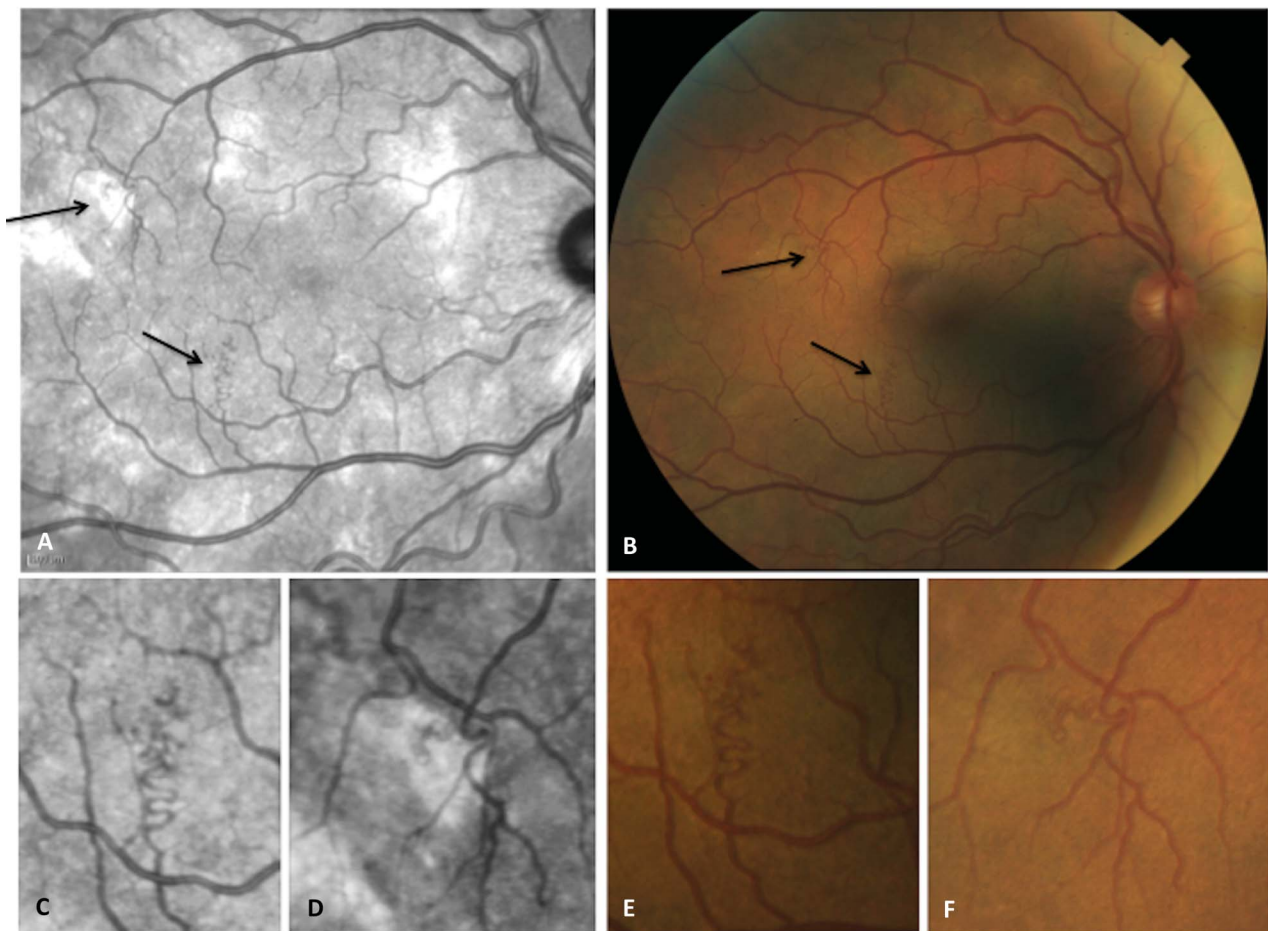

Fig. 1. Infrared image (**A**) and color fundus photography (**B**) of the right eye of a 14-year-old female showing multiple (two) retinal vascular abnormalities (RVAs) at the posterior pole (arrows). Only one of the two RVAs (the one localized along the upper temporal vascular arcade) is topographically located over an NF1-related choroidal abnormality visible in the IR image. High magnification IR (**C** and **D**) and color fundus (**E** and **F**) images are provided.
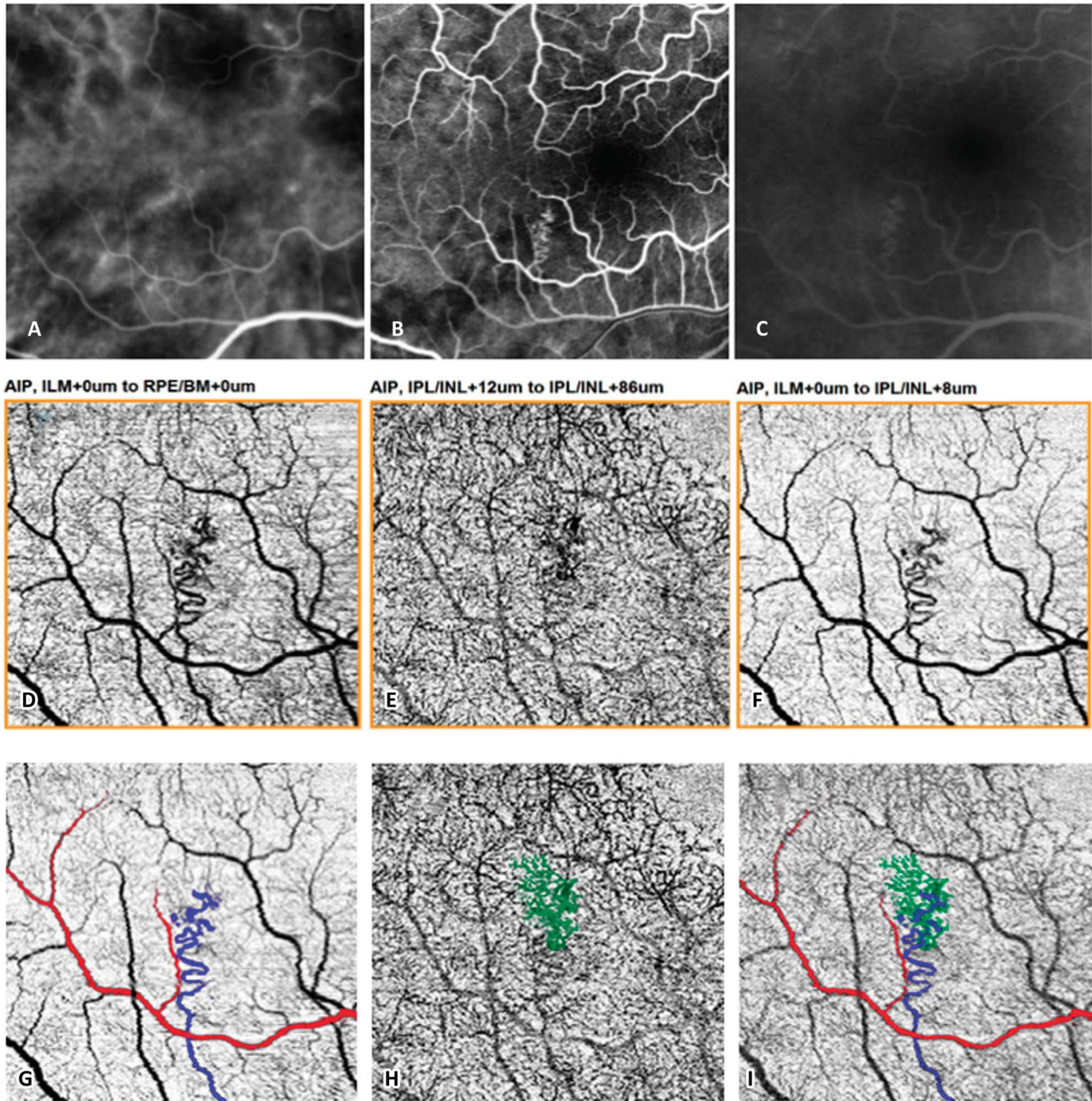
Fig. 2. Indocyanine green angiography, FA, and OCT-A of one of the two retinal vascular abnormalities (RVAs) of the case in Figure 1. The RVA is weakly visible in indocyanine green angiography and it is not topographically related to the NF1-related choroidal abnormalities located all around it (**A**). The RVA, detectable during the arteriovenous phase of the FA (**B**), is not characterized by any late intraretinal vascular leakage (**C**). The same RVA on OCT-A: at the en face image of the SCP. (**D**) The tortuous venule and the parallel normal profile arteriole were manually traced in purple and red, respectively (**G**). The en face image of the DCP (**E**) revealed the presence of localized anomalous crowded and congested capillary network (traced in green, **H**), which appeared to be located under or adjacent to the superficial anomalous venule on the en face image of the whole retina (**F**) and at the superimposition of the SCP and DCP en face images (**I**). AIP, advanced image processing; ILM, inner limiting membrane; RPE, retinal pigment epithelium; BM, Bruch membrane; IPL, inner plexiform layer; INL, inner nuclear layer.

instrument software. No manual adjustment was necessary. The 6 × 6 mm en face images were used to differentiate venules from arterioles. An arteriole is easily differentiated from a venule having a slightly smaller diameter than the corresponding venule, and because the arterioles are surrounded by a wider capillary-free zone.[17,18] The 3 × 3 mm en face images were used to analyze in detail the vascular networks.

Two independent observers examined the three different en face images obtained, both negative and positive images, of the full capillary bed, the SCP, and the DCP.

Using Photoshop CS6 (Adobe System Inc, San Jose, CA), for each RVA the courses of arterioles and venules were manually traced in the SCP plane. The convergence of deep capillaries into vortexes was also traced, and the 2 images were than superimposed (Figures 2 and 3).[17]

Statistical Analysis

The description of the analyzed population was performed according to the usual methods of descriptive statistics: frequency distribution and percentages, mean, SD, and range (minimum–maximum). The association between the presence of RVAs and other characteristics and parameters of the sampled population was assessed by chi-square or Fisher's exact tests. Comparison between patients with and without RVAs regarding age as well as average number of other concurrent NF1 signs was made by t-test for independent samples. Intergrader agreement was evaluated using Cohen's Kappa coefficient. All analyses were performed using SAS statistical software v.9.3 (SAS Institute, Cary, NC). A value of $P < 0.05$ was considered as statistically significant.

Results

Population and Neurofibromatosis Type 1 Diagnostic Criteria Analysis

Two hundred and 94 consecutive patients affected by NF1 were included in the study. Among these, 149 (50.7%) patients were female and 145 (49.3%) male. The demographic and clinical characteristics of the analyzed population, including race, iris color, and refractive errors, are reported in Table 1. The study group and the control group were similar in age, sex, race, iris color, and refractive status ($P > 0.05$). The

presence of NIH diagnostic criteria for NF1 was analyzed for both the NF1-affected group and the control group. Each diagnostic criterion was classified as follows: present, absent, or uninformative. None of the diagnostic criteria for NF1 was found in patients enrolled in the control group (including the presence of NF1-related choroidal abnormalities). Among the 294 affected patients, the diagnostic criteria were distributed as follows: 57 (19.4%) had 2 diagnostic criteria, 49 (16.7%) had 3 criteria, 76 (25.9%) had 4 criteria, 78 (26.5%) had 5 criteria, 32 (10.9%) had 6 criteria, and 2 (0.7%) had 7 criteria. The frequencies of each NF1 diagnostic criterion are reported in Table 2. Neurofibromatosis Type 1–related choroidal abnormalities (Table 2) and NF1-related systemic vascular abnormalities (Table 3) were detected in 186 (65.9%) and in 25 (9%) patients, respectively.

Retinal Vascular Abnormalities

The presence of RVAs was analyzed in both groups (NF1 affected and control group). Retinal vascular abnormalities were never observed in the control group; conversely, RVAs were detected in 18 (6.1%) of the 294 patients affected by NF1 (Figure 1). Of these, nine were female and seven were male ($P > 0.05$). Retinal vascular abnormalities were unilateral in 17 cases (94%), single in 15 (83.3%) cases, and multiple in 3 (16.7%) cases. Retinal vascular abnormalities were located at the posterior pole in 6 (33.3%) cases or along the temporal vascular arcades in 12 (66.6%). The interoperator agreement in the detection of RVAs was 1.0 (complete agreement). BL- and near-IR AF did not reveal any modification of normal (expected) fundus AF around these lesions. On FA, the RVAs were visible during the arteriovenous phase; no vascular late leakage or retinal vascular delay was present. A hyperfluorescence halo was

Table 1. Demographic and Clinical Characteristics of the Enrolled Patients

	NF1 affected, n = 294	Control group, n = 300	P
Mean age (years) ± SD	18.7 ± 15.2	18.9 ± 16.1	>0.05
Male/female, n (%)	149 (50.7)/145 (49.3)	141 (47)/159 (53)	>0.05
Iris color, n (%)			>0.05
Bright	98 (33.3)	94 (31)	
Dark brown	196 (66.7)	206 (69)	
Race, n (%)			>0.05
Non-Hispanic white	258 (87.8)	266 (89)	
Hispanic	11 (3.7)	12 (4.0)	
Black	12 (4.1)	12 (4.0)	
Others	13 (4.4)	10 (3.3)	
Refractive errors			>0.05
Myopia (>1 diopter)	56 (19)	46 (15)	
Astigmatism (>1 diopter)	50 (17)	55 (18)	
Hyperopia (>1 diopter)	69 (23)	61 (20)	

Table 2. Frequencies of Clinical Features in the NF1-Affected Group

	Data Available, n	Data Unavailable, n	Incidence, n (%)
Café-au-lait spots	275	19	273 (99.3)
Axillary or inguinal freckling	273	21	255 (93.4)
Lisch nodules	287	7	192 (66.9)
Neurofibromas	272	22	142 (52.2)
Family history of NF1	258	36	111 (43.0)
OPG	282	12	75 (26.6)
Distinctive osseous lesions	277	17	16 (5.8)
NF1-related choroidal abnormalities	282	12	186 (65.9)
NF1-RVAs	294	0	18 (6.1)

NF1-RVAs, NF1-related retinal vascular abnormalities.

detectable around the RVAs in FA in 75% of the cases in the arteriovenous phase, stable during the following phases (Figure 3). Each RVA identified by the IR imaging modality was visible by FA, and vice versa. Indocyanine green angiography did not reveal any leakage or other pathologic angiographic features related to the presence of RVAs (Figure 2).

Table 3. RVAs and Systemic Vascular Abnormalities Detected in Patients Affected by NF1

#	NF1-RVAs	Systemic Vascular Abnormalities
1	Yes	Severe stenosis of left renal artery; Moyamoya syndrome
2	Yes	Subretinal aortic stenosis
3	No	Cavernous angioma of left cerebellar hemisphere
4	No	Angioma of the neck
5	No	Vascular venous dysplasia of the neck with dilatation of the internal jugular vein
6	No	Diffuse angiomas in the trunk and limbs
7	No	Liver angioma
8	No	Hemangioma of the right lower limb
9	No	Right congenital common carotid artery stenosis (35%) and left parietal arteriovenous malformation
10	No	Spontaneous spleen rupture
11	No	Large carotid siphon aneurysm, kinking of the left internal carotid artery
12	No	Absence of left middle cerebral artery, internal carotid artery hypoplasia
13	No	Bone angioma
14	No	Renal angiomyolipoma
15	No	Angioma of the left chest wall
16	No	Right vertebral artery hypoplasia
17	No	Angioma of the right hip
18	No	Frontal and nape angiomas
19	No	Renal artery branch stenosis
20	No	Glomic tumor
21	No	Left renal artery dysplasia
22	No	Frontal and nape angiomas
23	No	Cutaneous flat angioma of the back
24	No	Bone angioma
25	No	Right intrarenal artery dysplasia

NF1-RVAs, NF1-related retinal vascular abnormalities.

The presence of RVAs did not specifically correlate with the following: patients age and sex ($P > 0.05$); the presence (age adjusted) of each single NF1 diagnostic criterion ($P > 0.05$); the number (age adjusted) of NF1 diagnostic criteria present in each patient ($P > 0.05$); the presence of NF1-related systemic vascular abnormalities ($P > 0.05$); and the presence and the location (Figure 1) of NF1-related choroidal abnormalities ($P > 0.05$) (Table 4). Eyes affected by RVAs show a normal visual acuity compared with age-based normative data in each case.

Optical Coherence Tomography Angiography Analysis

The en face image of the full capillary plexus was the superimposition of the SCP and DCP, and it gave an image close to that obtained with FA.

On the en face image of the SCP, the RVAs were characterized by a well-defined tortuous venule, parallel to a normal profile arteriole, with transverse capillaries, forming an interconnected plexus. In 75% of the cases, the en face image of the DCP revealed the presence of localized anomalous crowded and congested capillary network, under or adjacent to the superficial anomalous venule, connected to both the arteriole and the anomalous venule (Figure 3) In 30% of these cases, in which the deep capillary network was particularly congested and crowded, a light fluorescence was detectable around the RVAs by FA (Figure 3).

Discussion

Retinal vascular abnormalities have been reported in patients affected by NF1, but their frequency, diagnostic relevance, and pathologic implications still need to be clarified. Muci-Mendoza et al (2002) reported RVAs in 12 of the 32 patients (37.5%), whereas Abdolrahimzadeh et al (2014) reported RVAs in six of the 17 NF1 patients (35%).[12,13]
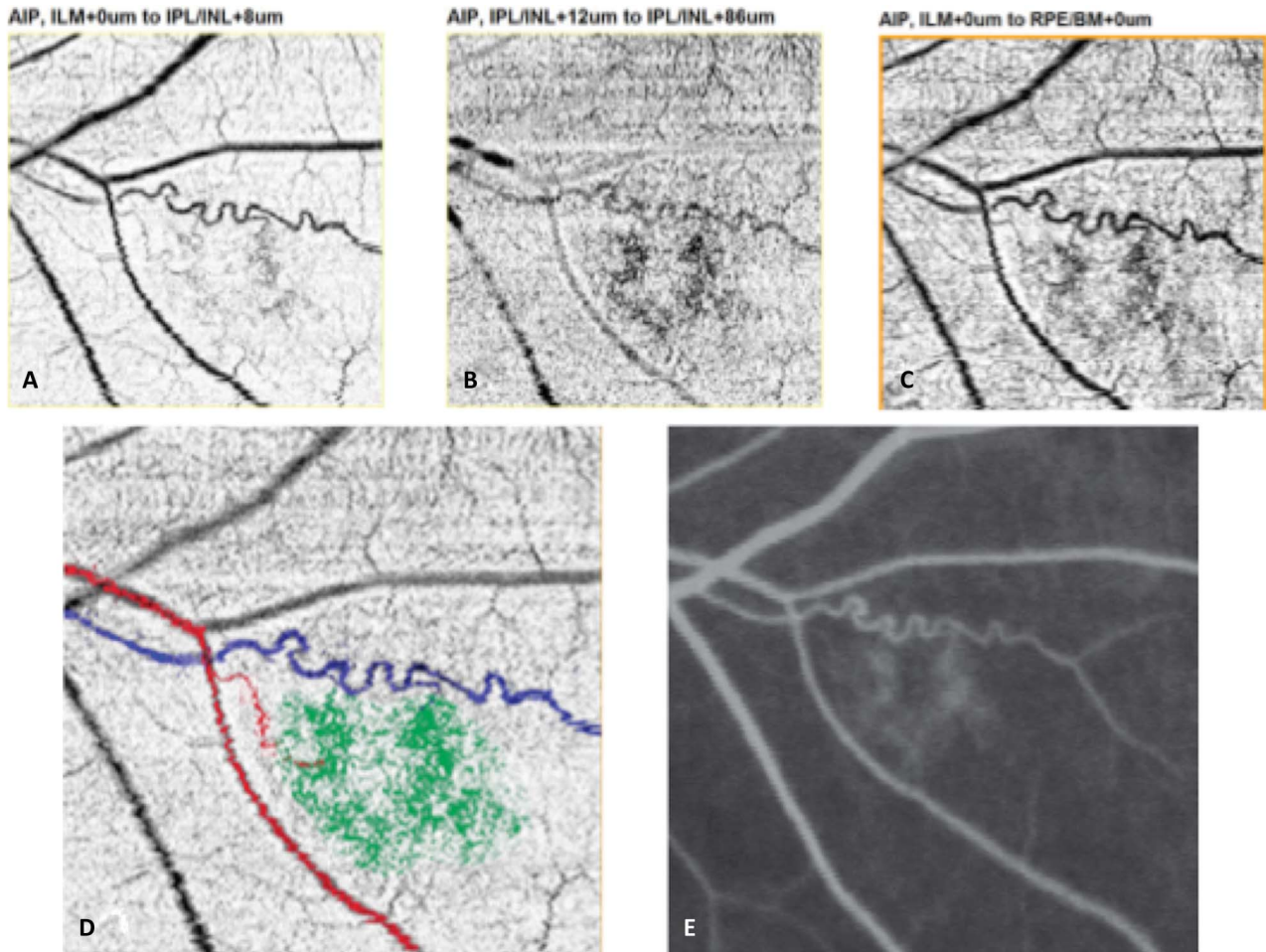
Fig. 3. Retinal vascular abnormalities (RVAs) in en face images of SCP (**A**), DCP, (**B**) and full retina (**C**) of OCT-A. The superimposition of the en face images of SCP and DCP (**D**) reveals the connection between the deep crowded capillaries network (green) to both the arteriole (red) and the anomalous venule (purple). A light fluorescence around the RVA is detectable on FA (**E**).

In this article, we have examined a cohort of 294 consecutive patients and evaluated the frequency of RVAs and their correlation with several clinical features. Compared with previously performed studies, we have identified RVAs in a smaller proportion of patients (6%). However, our study confirms that these abnormalities are a peculiar retinal vascular sign of this disease because they have been never documented in any of the aged-matched enrolled controls.

The presence of these signs did not correlate with age and sex, nor with any specific typical clinical signs of NF1; in particular, RVAs were not associated with other NF1 ocular signs (Lisch nodules and choroidal abnormalities), OPGs, nor systemic vascular abnormalities (including vascular stenosis/dysplasia/hypoplasia and angiomas). The lack of correlation between RVAs and NF1-related choroidal abnormalities partially disagrees with the study by Abdolrahimzadeh et al[13] (2014) who reported that RVAs overlay patchy choroidal alterations. Nevertheless, in our cohort, RVAs were not associated with the presence or the location of NF1-related choroidal abnormalities. Moreover, the lack of correlation between RVAs and systemic vascular abnormalities should be further investigated; of interest, the only patient affected by Moyamoya syndrome (patient one in Table 3), a rare and progressive cerebrovascular disorder caused by arteries occlusion in the basal ganglia, was also affected by RVAs.

The comparable proportion (50%) of patients with RVAs between minors and adults suggests that the vascular abnormalities might be congenital or early onset; however, follow-up studies could be helpful to confirm this hypothesis and to evaluate a possible delayed appearance of these retinal lesions or changes in preexisting ones.

The characteristics of RVAs in patients with NF1 are easily recognizable and well differentiated from retinal vascular signs reported in other pathologic conditions, as confirmed by the complete interobserver agreement obtained in this study. Indeed,

Table 4. Association Between NF1 Clinical Features and NF1-RVAs

	Presence of NF1-RVAs, P
Age	0.41
Sex	0.36
Café-au-lait spots	1.00
Axillary or inguinal freckling	1.00*
Lisch nodules	0.62†
Neurofibromas	0.84‡
Familiarity	0.17
OPG	1.00†
Distinctive osseous lesions	1.00
NF1-related choroidal abnormalities	0.48
Systemic vascular abnormalities	0.65

*including only subjects aged >5 years.
†including only subjects aged >8 years.
‡including only subjects aged >15 years.
NF1-RVAs, NF1-related retinal vascular abnormalities.

RVAs always appear as well-defined, small, tortuous vessels with a "spiral/corkscrew" aspect, originating in small tributaries of retinal veins, that is difficult to miss.[12,13] In addition, our study confirms that RVAs are not associated with any negative visual outcome for the patient. Therefore, although their specificity for the disease may suggest their possible inclusion among the diagnostic criteria of NF1, with the current knowledge, we do not recommend that patients should be screened for RVAs. In fact, current diagnostic criteria and molecular tests allow diagnosis of NF1 in the first years of life in most cases.

Using OCT-A, we were able to distinguish the different changes occurring in the retinal SCP and of the DCP associated with the RVAs. In many cases, the venous tortuous vessel, identified into the superficial retinal layers, was associated with specific localized vascular changes of the DCP. Histologic studies in animal models, and recently in human donors too, have demonstrated that the distribution of the microvascular network in the macula is complex, but follows a general theme, with some topographical and cellular structure properties of the human macular microvasculature that could be extremely valuable for understanding macular physiology and pathology.[18,19] The ability of OCT-A to display separately the SCP and the DCP has already been shown recently in normal subjects.[14–17] Spadie et al have demonstrated a laminar organization of the capillary plexus of the inner retina on OCT-A.[14] Savastano et al have also shown two different patterns of organization of the SCP and DSP.[15] Moreover, Bonnin et al[17] have recently demonstrated that the DCP is organized into polygonal units that converge into multiple capillary vortexes, located along the course of the superficial venules. The authors concluded that the capillary vortexes they described likely drain into the superficial venules.[17] In this study, we were able to confirm their hypothesis, observing drainage of the crowed anomalous DCP complex into a superficial venule. It is likely that the primary pathologic mechanism is the DCP changes, with the formation of crowded small vessels arising from the arterial side. The clinically visible venous anomaly of the corkscrew venules may be a secondary change in the draining venule due to the increased blood volume and pressure.

When the DCP changes were particularly evident by OCT-A, the venous tortuous vessel was surrounded by an anomalous fluorescent area on FA, detectable since the early capillary phase of the angiogram, with no angiographically detectable retinal capillaries and no changes in the late phase of the examination.

Two-dimensional FA imaging technique can explore the retina only on a single plane. In contrast, OCT-A provides a noninvasive approach for assessing the three-dimensional microcirculation of the retina.[14–21] Furthermore, our results confirm that OCT-A, being able to separately obtain images of the two major capillary networks of the retina (superficial and deep), shows vascular features and morphology that are not distinguishable with FA.[15] Our findings seem to confirm the hypothesis of Spaide et al,[14] that the diffuse fluorescence may be derived, in part, from the deeper capillary plexus and not only from the background choroidal fluorescence as usually ascribed. Moreover, the anomalous fluorescent area, detectable at FA, could be due to leaking DCP vessels.

Analyzing these findings from a systemic point of view, the possible correlation between RVAs and neurologic disorders such as epilepsy, headache, or intellectual disability in patients with NF1 is an extremely interesting field of research. Because retina is a part of the central nervous system and retinal and cerebral arterioles share similar anatomy, physiology, and embryology, it is likely that patients with RVAs may also have cerebral microvascular abnormalities. Although we were unable to identify an association with any neurologic deficit in the subgroup of patients affected by RVAs, future studies are warranted to explore this idea more deeply.

In conclusion, RVAs are present in a moderate proportion of patients affected by NF1 and can be considered an additional distinctive sign of the disease. The presence of these lesions did not affect visual acuity and did not correlate with known specific ocular or systemic NF1 features. Optical coherence tomography angiography can detect two morphologic RVA features differently involving the superficial and the deep retinal vascular plexus.

Acknowledgments

References

1. Payment E, Vidaud M, Vidaud D, Wolkenstein P. Neurofibromatosis type 1: from genotype to phenotype. J Med Genet 2012;49:483–489.

2. Evans D, Howard E, Giblin C, et al. Birth incidence and prevalence of tumor-prone syndromes: estimates from a UK family genetic register service. Am J Med Genet A 2010;152:327–332.

3. National Institutes of Health Consensus Development Conference Statement: neurofibromatosis. Bethesda, Md., USA, July 13–15, 1987. Neurofibromatosis 1988;1:172–178.

4. Tadini G, Milani D, Menni F, et al. Is it time to change the neurofibromatosis 1 diagnostic criteria? Eur J Intern Med 2014;25:506–510.

5. Parrozzani R, Clementi M, Frizziero L, et al. In vivo detection of choroidal abnormalities related to NF1: feasibility and comparison with standard NIH diagnostic criteria in pediatric patients. Invest Ophthalmol Vis Sci 2015;56:6036–6042.

6. Parrozzani R, Clementi M, Kotsafti O, et al. Optical coherence tomography in the diagnosis of optic pathway gliomas. Invest Ophthalmol Vis Sci 2013;54:8112–8118.

7. Vagge A, Camicione P, Capris C, et al. Choroidal abnormalities in neurofibromatosis type 1 detected by near-infrared reflectance imaging in paediatric population. Acta Ophthalmol 2015;93:667–671.

8. Viola F, Villani E, Natacci F, et al. Choroidal abnormalities detected by near-infrared reflectance imaging as a new diagnostic criterion for neurofibromatosis 1. Ophthalmology 2012;119:369–375.

9. Hodgson N, Kinori M, Goldbaum MH, Robbins SL. Ophthalmic manifestations of tuberous sclerosis: a review. Clin Exp Ophthalmol 2017;45:81–86.

10. Mantelli F, Bruscolini A, La Cava M, et al. Ocular manifestations of Sturge-Weber syndrome: pathogenesis, diagnosis, and management. Clin Ophthalmol 2016;10:871–878.

11. Haddad NM, Cavallerano JD, Silva PS. Von hippel-lindau disease: a genetic and clinical review. Semin Ophthalmol 2013;28:377–386.

12. Muci-Mendoza R, Ramella M, Fuenmayor R. Corkscrew retinal vessels in neurofibromatosis type 1: report of 12 cases. Br J Opthalmol 2002;86:282–284.

13. Abdolrahimzadeh S, Felli L, Piraino DC, et al. Retinal microvascular abnormalities overlying choroidal nodules in neurofibromatosis type 1. BMC Ophthalmol 2014;14:146.

14. Spaide RF, Klancnik JM Jr, Cooney MJ. Retinal vascular layers imaged by fluorescein angiography and optical coherence tomography angiography. JAMA Ophthalmol 2015;133:45–50.

15. Savastano MC, Lumbroso B, Rispoli M. In vivo characterization of retinal vascularization morphology using optical coherence tomography angiography. Retina 2015;35:2196–2203.

16. Al-Sheikh M, Tepelus TC, Nazikyan T, Sadda SR. Repeatability of automated vessel density measurements using optical coherence tomography angiography. Br J Ophthalmol 2016;0:1–4.

17. Bonnin S, Mané V, Counturier A, et al. New insight into the macular deep vascular plexus imaged by optical coherence tomography angiography. Retina 2015;35:2347–2352.

18. Yu PK, Balaratnasingam C, Cringle SJ, et al. Microstructure and network organization of the microvasculature in the human macula. Invest Ophthalmol Vis Sci 2010;51:6735–6743.

19. Snodderly DM, Weinhaus RS, Choi JC. Neural-vascular relationships in central retina of macaque monkeys (Macaca fascicularis). J Neurosci 1992;12:1169–1193.

20. Jia Y, Bailey ST, Wilson DJ, et al. Quantitative optical coherence tomography angiography of choroidal neovascularization in age-related macular degeneration. Ophthalmology 2014;121:1435–1444.

21. Weinhaus RS, Burke JM, Delori FC, Snodderly DM. Comparison of fluorescein angiography with microvascular anatomy of macaque retinas. Exp Eye Res 1995;61:1–16.